Radiation Efficiency of the Spherical Metallic Nanoparticles, Covered with Molecular Adsorbate Layer

A.V. Korotun[1,2,*], N.A. Smirnova[1], G.V. Moroz[1], G.M. Shilo[3]

[1] *Zaporizhzhia Polytechnic National University, 64, Zhukovsky st., 69063 Zaporizhzhia, Ukraine*
[2] *G.V. Kurdyumov Institute for Metal Physics, N.A.S. of Ukraine, 36 Academician Vernadsky blvd., 03142 Kyiv, Ukraine*
[3] *Zaporizhzhia National University 66, Zhukovsky st., 69600 Zaporizhzhia, Ukraine*

The relations for the optical characteristics of the composite nanoparticles of the type "metallic core – molecular aggregate shell" have been obtained in the work. The calculations of the frequency dependencies of the polarizability, absorption and scattering cross-sections, radiation efficiency and size dependencies of the frequencies of the hybrid plasmon-exciton resonances have been performed. An approximate approach to the determination of the size dependencies of the frequencies of the hybrid plasmon-exciton modes, the essence of which is to ignore the relaxation processes in the molecular aggregate shell and in metallic core, has been proposed. It has been demonstrated that the increase in the radius of metallic core results in the decrease in the highest frequency of plasmon-exciton resonance, while the next highest frequency increases. At the same time, the smallest of these frequencies decreases first, and when the content of metallic fraction becomes greater that 50 % of the volume of the entire particle, it begins to increase. The evolution of the maximums of the imaginary part of the polarizability with the change of the geometric parameters of the composite nanoparticle: the radius of metallic core and the thickness of the shell has been observed. It has been established that one of these maximums is situated in the near ultraviolet region, whereas the other two of them are in the visible part of the spectrum. Moreover, it should be pointed out the significant increase in the real and imaginary parts and the module of the polarizability under the increase in the radius of metallic core. The necessity of taking into account both absorption and scattering under the study of the optical properties of nanoparticles of the composition "metallic core – J-aggregate" is proved. It has been shown that the value of radiation efficiency in the optical frequency range is practically independent on the changes of the thickness and material of the shell, while the change of material and radius of metallic core has significant effect on its frequency dependence in the visible part of the spectrum. The feasibility of the practical use of the composite nanoparticles with golden core with the small radius, in which the radiation efficiency is close to one in the entire optical frequency range, has been established.

Keywords: Composite nanoparticle, Plasmon-exciton resonance, Molecular adsorbate, Relaxation rate, Frequency dependencies.

1. INTRODUCTION

The metallic nanoparticles in combination with molecular adsorbates are one of the most adapted architectures for the development and implementation of the different functions on the nanoscale. For example, the complexes "metallic nanoparticle – molecular adsorbate" are used as nanoscale acidity meters [1], light harvesters [2] and optically sensitive active nanocomplexes [3,4]. The main reason for the widespread use of such systems is associated with the variety of the mechanisms of interaction between the surface of metallic nanoparticles and molecular adsorbates. It is known that adsorbate molecules can change the optical properties of nanoparticles by shifting their surface plasmonic resonance [5] or by imparting ferromagnetism at room temperature to usually nonmagnetic nanoparticles [6]. At the same time, the properties of adsorbates, such as fluorescence, can be suppressed or enhanced in the presence of metallic nanoparticles. Thus, the interaction between the nanoparticles and molecular adsorbates can results in the formation of the strongly bound complexes based on the nanoparticles with the unique optical characteristics [7], which differ both from the

properties of the individual nanoparticles and molecular adsorbates.

Many types of the interaction between metallic nanoparticles and molecular adsorbates are based on the collective electron oscillations – localized surface plasmons, which take place in metallic nanoparticles [8-10]. Localized surface plasmons are confined in space and significantly enhance the fields on the surface of nanoparticles compared to the field of an incident light wave. This enhanced near field significantly changes the properties of molecules, molecular complexes, or other exciton systems. In the case of the strong and coherent plasmon-exciton coupling, the properties of both plasmon and exciton are modified by their interaction. A number of experiments have observed strong plasmon-exciton coupling in metal films with propagating plasmons [11], and in particles of complex geometries, where both localized and propagating plasmons contribute to the total system interaction [12,13]. For example, a coherent plasmon-exciton coupling was found between localized plasmons in Ag nanospheres and excitons in molecular J-aggregates [14]. J-aggregates are organic semiconductors with excitons which interact with an intense near field of localized surface plasmons. The strong interaction of J-aggregate excitons with plasmons

---

* andko@zp.edu.ua

[15] and photons [16] results in the formation of mixed states. In such systems, the ultrafast dynamical properties of J-aggregates are strongly modified. The interaction between excitons and photons has been studied for J-aggregates in microresonators [17], and more recently for J-aggregates which interact with surface plasmons propagating on extended metal structures (metal films) [18]. However, the dynamic response of excitons of J-aggregates, associated with localized plasmons of nanoparticles, has not been directly investigated so far. The ultrafast properties of metal nanoparticle – J-aggregate complexes have been reported for the case when the transition energy of the J-aggregate is strongly mismatched with respect to the energy of the resonant plasmon [19]; however, this is a weaker mode of interaction, which differs significantly from the stronger interactions in the double resonance mode. In the weaker, non-resonant mode, plasmon – molecule interaction usually results in the increase in molecular absorption and in the shift of plasmon resonance frequency. Fundamentally new effects occur under the strong interaction between localized plasmons and excitons, when hybridization takes place and plexitons are formed, whose behavior differs from both plasmons and excitons [20]. As has been recently shown, in a number of plasmonic systems, strong coupling between metal nanoparticles can result in Fano interference and resonances [21]. Such interference can also occur in hybrid systems "metallic nanoparticle – semiconductor quantum dot", where the coupling between excitons and plasmons can also lead to an enhancement of Fano effect [22].

Thus, hybrid molecular-plasmonic nanostructures provide the promising strategy for the development of active nonlinear materials at optical frequencies [23,24]. Studies of ultrafast optical interactions in the time domain can show how these interactions lead to new properties and how processes such as plasmon-exciton hybridization, energy or charge transfer can contribute into the response of a new hybrid material.

In this regard, the study of the spectral properties of hybrid Me@J nanostructures and the effects arising from their interaction with optical radiation are of considerable interest for various applications, including biology and the development of organic LEDs, photodetectors, and solar cells [10,25-28].

Therefore, the purpose of this work is to study the optical response of the hybrid resonant plasmon-exciton system consisting of the complex "metallic nanoparticle – J-aggregate".
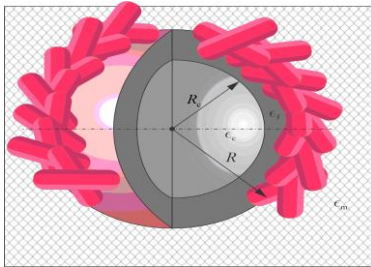
2. BASIC RELATIONS

Fig. 1 – Geometry of the problem

Let us consider the spherical metallic nanoparticle with the radius R_c, covered with J-aggregate layer with the thickness t, which is situated in medium with the permittivity ϵ_m and has the total radius $R = R_c + t$ (Fig. 1).

The radiation efficiency, which is determined by the following relation [29,30], is an important optical characteristics of metallic composite nanoparticles

$$\xi_@^{rad} = \frac{1}{1 + C_@^{abs}/C_@^{sca}}, \tag{1}$$

it is proportional to the ratio of energy of the electromagnetic field, scattering by nanoparticles, to energy of the incident electromagnetic wave.

In formula (1) the values $C_@^{abs}$ and $C_@^{sca}$ are the absorption and scattering cross-sections, which are under the study in optical experiments, they are determined in dipole approximation by the polarizability of the nanoparticles

$$C_@^{abs} = \frac{\omega}{c}\sqrt{\epsilon_m}\,\mathrm{Im}\,\alpha_@, \tag{2}$$

$$C_@^{sca} = \frac{\omega^4}{6\pi c^4}\epsilon_m^2|\alpha_@|^2, \tag{3}$$

where c is the velocity of light, ω is the frequency of the incident electromagnetic wave.

Dipole polarizability of such composite nanoparticle $\alpha_@$ determines, in fact, all the particularities of the interaction between electromagnetic waves and composite nanoparticles and is determined by the relation

$$\alpha_@ = R^3\frac{\epsilon_@ - \epsilon_m}{\epsilon_@ + 2\epsilon_m}, \tag{4}$$

where the dielectric function of two-layer nanoparticle has the form [30–32]

$$\epsilon_@ = \epsilon_J\frac{1 + 2\beta_c\delta_@}{1 - \beta_c\delta_@}, \tag{5}$$

and

$$\delta_@ = \frac{\epsilon_c - \epsilon_J}{\epsilon_c + 2\epsilon_J}. \tag{6}$$

In formulas (5) and (6) $\beta_c = (R_c/R)^3$ is the volume fraction of metal in the composite nanoparticle, and the dielectric functions of materials of the core and shell have the form, correspondingly:

$$\epsilon_c(\omega) = \epsilon^\infty - \frac{\omega_p^2}{\omega(\omega + i\gamma_{eff})}, \tag{7}$$

$$\epsilon_J(\omega) = \epsilon_J^\infty + \frac{f\omega_0^2}{\omega_0^2 - \omega^2 - i\omega\gamma_J}, \tag{8}$$

where ω_p is the plasma frequency; ϵ^∞ is the contribution of the crystal lattice into the dielectric function of metallic core; f is the reduced oscillator force; ϵ_J^∞ is the value of the dielectric permittivity away from the center of the absorption J-stripe; ω_0 is the frequency, which corresponds to the center of the stripe, γ_J is the width of Lorentzian contour of J-stripe.

In formula (7) the effective relaxation rate in the nanoparticles γ_{eff} is determined by the sum of the contributions of bulk γ_{bulk} and surface relaxation γ_s and radiation damping γ_{rad} [33]

$$\gamma_{eff} = \gamma_{bulk} + \gamma_s + \gamma_{rad}. \tag{9}$$

Bulk relaxation rate is constant, the radiation damping for the particles of the considered sizes can be ignored, and the surface relaxation rate depends on both the frequency and the size of the particles [34]

$$\gamma_s = \mathscr{A}\left(\omega, R\right)\frac{v_F}{R_c}, \qquad (10)$$

where v_F – Fermi electron velocity, and the effective parameter of the coherence loss for the spherical nanoparticles has the form [35]

$$\mathscr{A}\left(\omega, R\right) = \frac{1}{4}\left(\frac{\omega_p}{\omega}\right)^2\left[1 - \frac{2v_s}{\omega}\sin\frac{\omega}{v_s} + \frac{2v_s^2}{\omega^2}\left(1 - \cos\frac{\omega}{v_s}\right)\right], \quad (11)$$

$v_s = v_F/2R_c$ is the frequency of the individual oscillations of electrons.

Thereafter, the relations (1) – (4) taking into account expressions (5) – (11) are going to be used for the obtaining of the numerical results.

3. THE RESULTS OF THE CALCULATIONS AND THEIR DISCUSSION

The calculations of the frequency dependencies of the polarizability, light absorption and scattering cross-sections and radiation efficiency have been performed for the particles of the different size and content. The parameters of metals and cyanine dyes are given in Tables 1 and 2 correspondingly.

Table 1 – The parameters of metals (a_0 − Bohr radius) (see, for example, [32, 34] and references therein)

Value	Metals			
	Cu	Au	Ag	Pt
r_s/a_0	2.11	3.01	3.02	3.27
m^*/m_e	1.49	0.99	0.96	0.54
ϵ^∞	12,03	9,84	3,7	4,42
$\gamma_{bulk}, 10^{14}\ s^{-1}$	0.37	0.35	0.25	1.05

Table 2 – The parameters of J-aggregates (see, for example, [36] and references therein).

Value	J-aggregates		
	TC	OC	PIC
ϵ_J^∞	1	1	2.9
$\hbar\omega_0,\ eV$	2.68	3.04	2.13
f	0.90	0.01	0.10
$\hbar\gamma_J,\ eV$	0.066	0.039	0.033

Fig. 2 shows the frequency dependencies for the real and imaginary parts, and for the module of the polarizability for nanoparticles Au@TC with the variable thickness of the shell and the constant radius of metallic core. It should be pointed out that $\mathrm{Re}\alpha_@(\omega)$ is an alternating function of frequency (Fig. 2*a*), whereas $\mathrm{Im}\alpha_@(\omega) > 0$ throughout the entire frequency range which is under the study (Fig. 2*b*). The curves $|\alpha_@(\omega)|$ are qualitatively and quantitatively close to the curves $\mathrm{Im}\alpha_@(\omega)$. Moreover, if the first and the second

maximums $\mathrm{Im}\alpha_@(\omega)$ and $|\alpha_@(\omega)|$ are situated in the visible part of the spectrum, then the third maximum – in the near ultraviolet range. The increase in the thickness of the shell results in the increase in values of all maximums and in slight "red" shifts of the first and the third maximums and "blue" shift of the second maximum.
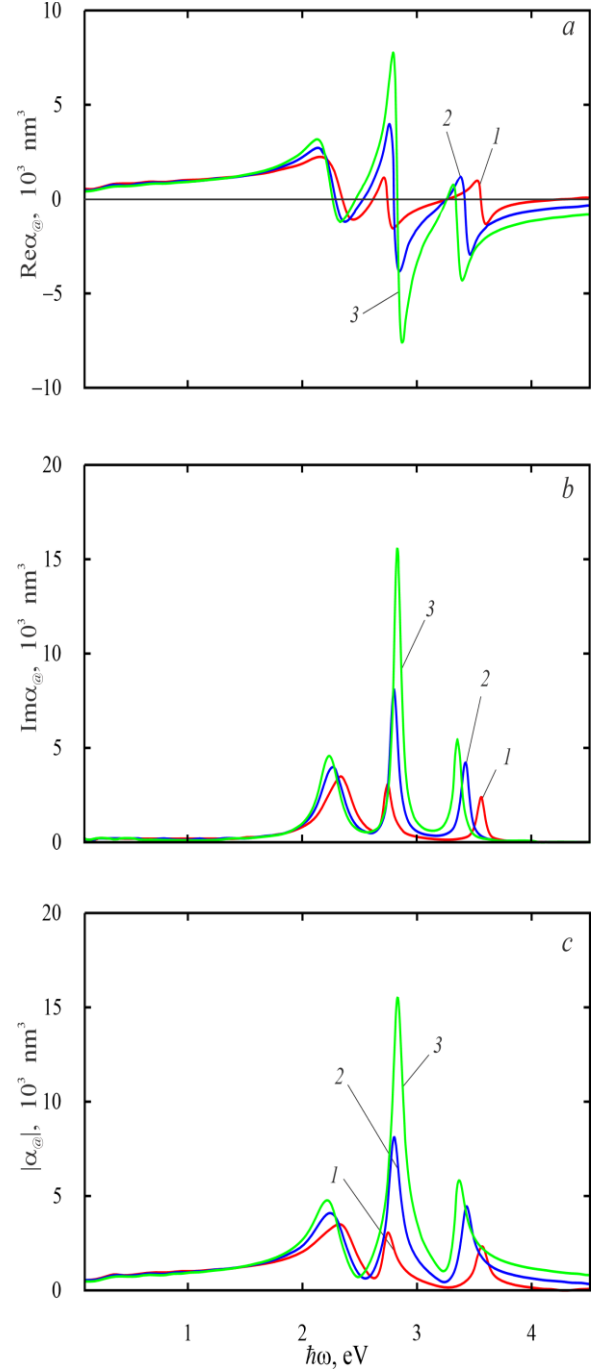

Fig. 2 – The frequency dependencies for the real (*a*) and imaginary (*b*) parts, and module (*c*) of the polarizability of the composite nanoparticles Au@TC ($R_c = 10$ nm) under the dirrerent thickness of the shell: *1* − $t = 1$ nm ; *2* − $t = 3$ nm ; *3* − $t = 5$ nm

Fig. 3 shows the similar to the previous figure dependencies for the particles Au@TC with the different

radius of metallic core and constant thickness of the shell. Let us point out that the increase in the radius of metallic core results in the significant increase in values of $\mathrm{Re}\,\alpha_@$, $\mathrm{Im}\,\alpha_@$ and, correspondingly, $|\alpha_@|$, which is associated with the increase in the content of metallic fraction in nanoparticle. Small-scale oscillations in the infrared region of the spectrum on the dependencies $\mathrm{Im}\,\alpha_@(\omega)$ can be explained by the influence of the kinetic effects. Let us point out that the number of maximums $\mathrm{Im}\,\alpha_@(\omega)$ is the same as in the previous case, and their location is constant under the variation of the radius of the core.

Let us point out that maximums $\mathrm{Im}\,\alpha_@(\omega)$ correspond to the hybrid plasmon-exciton resonances, the frequencies of which $\omega_{\mathrm{res}}^{(i)}$ ($i = 1, 2, 3$) are determined from the condition

$$\mathrm{Re}\,\epsilon_@\left(\omega_{\mathrm{res}}^{(i)}\right) + 2\epsilon_{\mathrm{m}} = 0 \ . \tag{12}$$

An approximate analytic approach to the determination of these frequencies is to assume that the relaxation processes in metallic core and the shell of J-aggregate can be ignored (that is, one can assume $\gamma_{\mathrm{eff}} = \gamma_{\mathrm{J}} = 0$).

Let us give the numerical results for the frequencies $\omega_{\mathrm{res}}^{(i)}$ for the particles Au@TC and Ag@TC under the different values of the content of metal in the particle (Table 3).

Let us point out that the increase in content of metallic fraction results in the decrease in resonant frequencies $\omega_{\mathrm{res}}^{(1)}$ for both particles Au@TC and particles Ag@TC, while the frequencies $\omega_{\mathrm{res}}^{(2)}$ increase on the contrary. As for the frequencies $\omega_{\mathrm{res}}^{(3)}$, it should be pointed out the following: these frequencies both for the particles Au@TC and the particles Ag@TC first decrease with the increase in β_{c}, and then (at $\beta_{\mathrm{c}} > 0.5$) begin to increase. Moreover, if the frequencies $\omega_{\mathrm{res}}^{(2)}$ and $\omega_{\mathrm{res}}^{(3)}$ belong to the optical frequency range, then the frequencies $\omega_{\mathrm{res}}^{(1)}$ are situated in ultraviolet part of the spectrum.
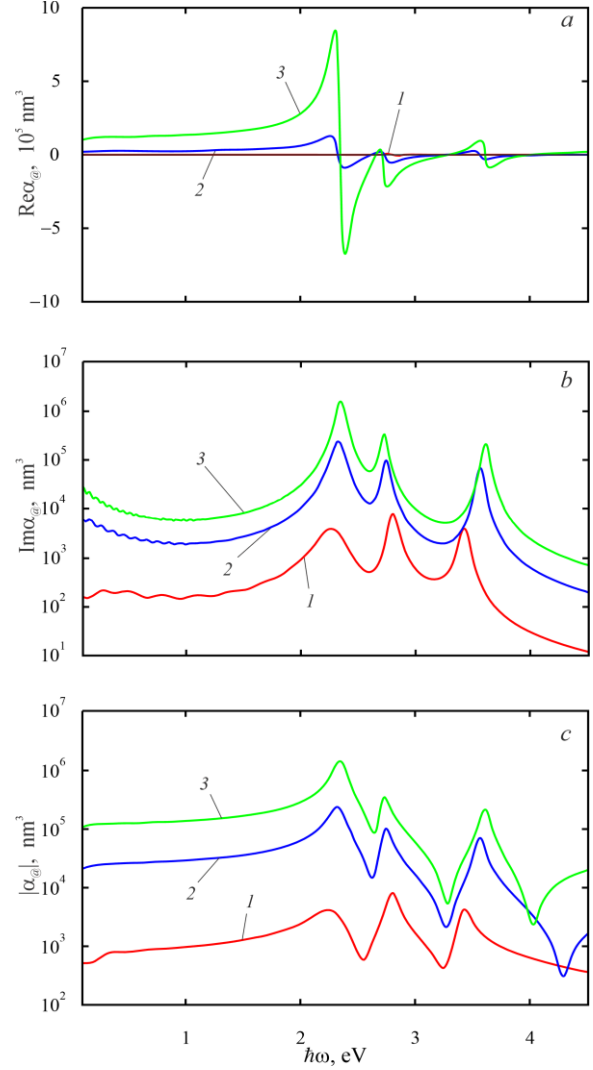

Fig. 3 – The frequency dependencies for the real (*a*) and imaginary (*b*) parts, and module (*c*) of the polarizability of the composite nanoparticles Au@TC ($t = 3\,\mathrm{nm}$) with the different radius of the core: *1* – $R_{\mathrm{c}} = 10\,\mathrm{nm}$; *2* – $R_{\mathrm{c}} = 30\,\mathrm{nm}$; *3* – $R_{\mathrm{c}} = 50\,\mathrm{nm}$

Table 3 – The calculated values of the resonant frequencies for the nanoparticles Au@TC

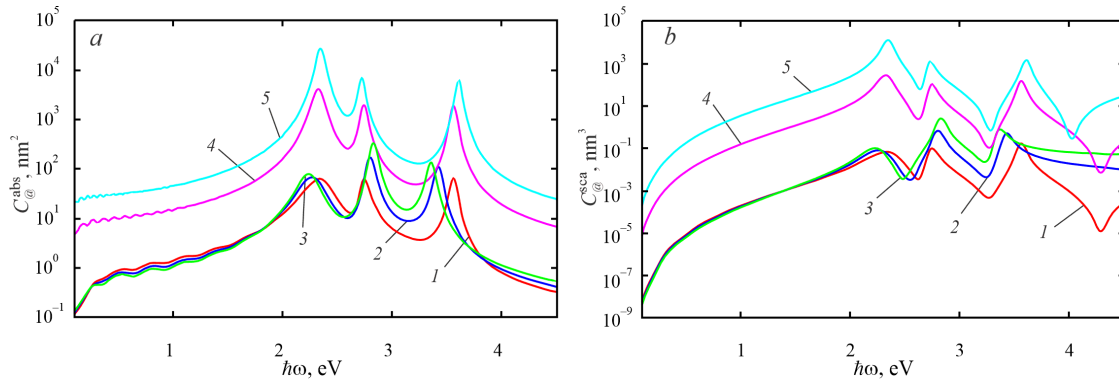| β_{c}	Au@TC			Ag@TC		
	$\hbar\omega_{\mathrm{res}}^{(1)}$, eV	$\hbar\omega_{\mathrm{res}}^{(2)}$, eV	$\hbar\omega_{\mathrm{res}}^{(3)}$, eV	$\hbar\omega_{\mathrm{res}}^{(1)}$, eV	$\hbar\omega_{\mathrm{res}}^{(2)}$, eV	$\hbar\omega_{\mathrm{res}}^{(3)}$, eV
0.1	6.851	2.258	1.859	6.247	2.523	2.255
0.2	6.471	2.417	1.718	6.011	2.651	2.166
0.3	6.116	2.538	1.622	5.773	2.756	2.105
0.4	5.772	2.629	1.574	5.532	2.843	2.075
0.5	5.438	2.697	1.573	5.286	2.914	2.076
0.6	5.110	2.745	1.617	5.031	2.971	2.111
0.7	4.781	2.779	1.705	4.765	3.015	2.182
0.8	4.445	2.799	1.835	4.777	3.048	2.295
0.9	4.087	2.809	2.014	4.151	3.073	2.462

Fig. 4 – The frequency dependencies for the absorption cross-section (*a*) and scattering cross-section (*b*) of the composite nanoparticles Au@TC: *1 –* $R_c = 10$ nm , $t = 1$ nm ; *2 –* $R_c = 10$ nm , $t = 3$ nm ; *3 –* $R_c = 10$ nm , $t = 3$ nm ; *4 –* $R_c = 30$ nm , $t = 3$ nm ; *5 –* $R_c = 50$ nm , $t = 3$ nm
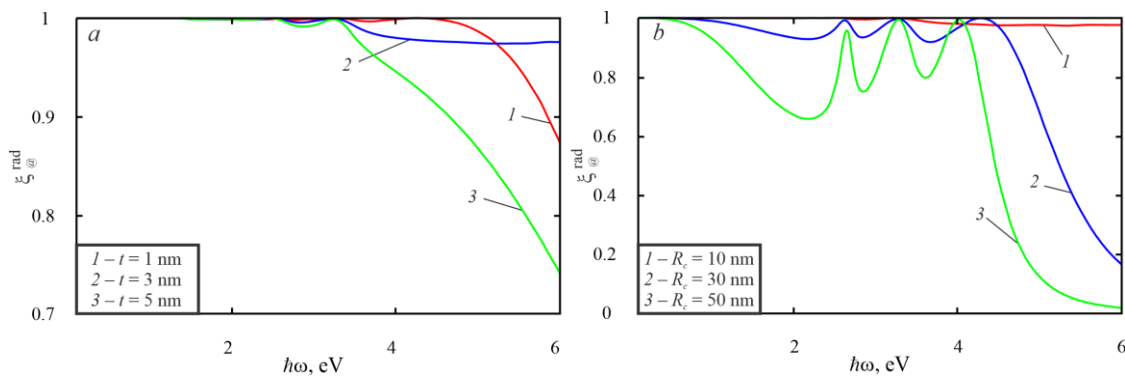

Fig. 5 – The frequency dependencies for the radiation efficiency of the composite nanoparticles Au@TC with the different thickness of the shell under $R_c = 10$ nm (*a*) and the different radius of metallic core under $t = 3$ nm (*b*)
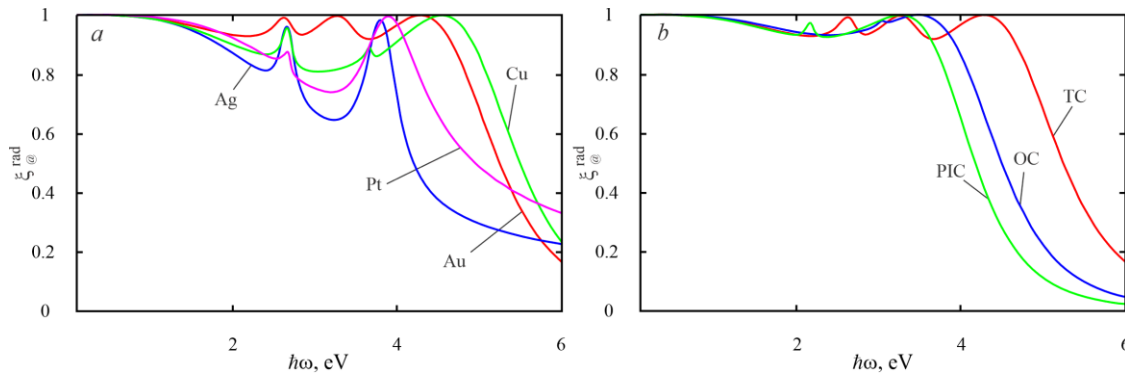

Fig. 6 – The frequency dependencies for the radiation efficiency of the composite nanoparticles Me@TC under the variation of material of the core (*a*) and composite nanoparticles Au@J (*b*) under the variation of material of the shell ($R_c = 30$ nm , $t = 3$ nm)

The calculations of the frequency dependencies for the absorption and scattering cross-sections (Figure 4) indicate their qualitative similarity to the similar dependencies for $\operatorname{Im}\alpha_@(\omega)$ and $|\alpha_@(\omega)|$. This applies to both the number of maximums and the evolution of their position and magnitude. Thus, when the radius of the core changes, the position of the maxima does not change, but their magnitude increases; when the thickness of the shell changes, on the contrary, the amplitude of the maxima practically does not change, but their "red" and "blue" shifts (depending on the maximum number) in frequency occur. It can also be

pointed out that $C_@^{\mathrm{abs}}$ and $C_@^{\mathrm{sca}}$ coincide in the order of magnitude, which indicates the importance of taking into account both absorption and scattering for the study of the hybrid nanostructures.

Fig. 5 shows the frequency dependencies for the radiation efficiency of the nanoparticles Au@TC with the different thickness of the shell and the different radius of the core. The results of the calculations indicate that the variation of the thickness of the shell has virtually no effect on the radiation efficiency in the optical frequency range, and in the ultraviolet part of the spectrum $\xi_@^{\mathrm{rad}}$ decreases more intensively for the

particles with the thicker shell.

In turn, the variation of the radius of metallic core has the significant effect on the frequency dependence of the radiation efficiency. For example, for the particles with the relatively large radius of the core, the value $\xi_@^{rad}$ decreases essentially already in the optical frequency range, which is undesirable in the practical application of the studied nanoobjects. At the same time, the radiation efficiency of the composite particles with the relatively small radius of the core is close to one, which indicates the feasibility of the practical use of such nanoparticles.

Fig. 6 shows the frequency dependencies of the radiation efficiency for the nanoparticles with the shells and cores of different materials. An analysis of the numerical results indicates that the variation of metal of the core has the significant effect on the value of the radiation efficiency in the optical frequency range (Figure 6, *a*), while the variation of J-aggregate of the shell has the influence on the radiation efficiency only under the great frequencies (Figure 6, *b*). Moreover, the value $\xi_@^{rad}$ is the greatest value for the composite particles with the core Au in the visible part of the spectrum.

4. CONCLUSIONS

The relations for the frequency dependencies for the polarizability, resonant frequencies, absorption and scattering cross-sections and radiation efficiency of the spherical nanoparticles "metallic core – J-aggregate shell" have been obtained.

It has been established that the curves of the imaginary part of the polarizability have three maximums, which correspond to the frequencies of the hybrid plasmon-exciton resonance. It has been shown that the amplitude of these maximums increases with the increase in the radius of the core, while the shifts of the maximums take place under the variation of the thickness of the shell.

It has been shown that the behavior of the hybrid frequencies of plasmon-exciton resonances is the same in the case of different materials of the core and is determined by the bulk content of metallic fraction in the particle.

It has been proved that the absorption and scattering cross-sections are close in value, hence, both these processes should be taken into account under the studies.

It has been established that the variation of the thickness of the shell, as well as the variation of its material, do not affect the radiation efficiency of nanoparticles in the optical frequency range, while the radiation efficiency changes greatly under the variation of material and the sizes of the core.

Since the value of the radiation efficiency in the optical frequency range is close to one for the particles with golden core of the small radius, then such nanoparticles should be used to obtain maximum radiation efficiency.

REFERENCES

1. S.W. Bishnoi, C. Rozell, C.S. Levin, M.K. Gheith, B.R. Johnson, D.H. Johnson, N.J. Halas, *Nano Lett.* **6**, 1687 (2006).
2. A.O. Govorov, I. Carmeli, *Nano Lett.* **7**, 620 (2007).
3. N. Haberkorn, M.C. Lechmann, B.H. Sohn, K. Char, J.S. Gutmann, P. Theato, *Macromol. Rapid Commun.* **30** No 14, 1146 (2009).
4. Y. Yamanoi, T. Nakae, H. Nishihara, *Chem. Lett.* **50** No 6, 1263 (2021).
5. N.A. Smirnova, A.V. Korotun, I.M. Titov, *Him. Fiz. Tehnol. Poverhni.* **13** No 4, 476 (2022).
6. P. Crespo, R. Litran, T.C. Rojas, M. Multigner, J.M. de la Fuente, J.C. Sanchez-Lopez, M.A. Garcia, A. Hernando, S. Penades, A. Fernandez, *Phys. Rev. Lett.* **93** No 8, 087204 (2004).
7. J.M. García-Martínez, E.P. Collar, *Polymers* **13** No 15, 2390 (2021).
8. N.L. Dmitruk, S.Z. Malynych, I.E. Moroz, *J. Nano-Electron. Phys.* **5** No 3, 03031 (2013).
9. J. Boken, P. Khurana, S. Thatai, D. Kumar, S. Prasad, *Appl. Spectrosc. Rev.* **52** No 9, 774 (2017).
10. A.O. Koval, A.V. Korotun, Yu.A. Kunytskyi, V.A. Tatarenko, I.M. Titov, *Electrodynamics of Plasmon Effects in Nanomaterials* (Kyiv: Naukova Dumka: 2021) (in Ukrainian).
11. M. Rödel, P. Lisinetskaya, M. Rudloff, M. Stark, J. Manara, R. Mitric, J. Pflaum, *J. Phys. Chem. C.* **126** No 8, 4163 (2022).
12. G. Zengin, G. Johansson, P. Johansson, T.J. Antosiewicz, M. Käll, T. Shegai, *Sci. Rep.* **3**, 3074 (2013).
13. Z. He, F. Li, P. Zuo, C. Xu, W. He, J. He, Y. Zhou, Q. Zhang, K. Chen, H. Huang, L. Hu, *J. Phys. Chem. C.* **126** No 40, 17141 (2022).
14. S.I. Azzam, A.V. Kildishev, R.-M. Ma, C.-Z. Ning, R. Oulton, V.M. Shalaev, M.I. Stockman, J.-L. Xu, X. Zhang, *Light Sci.*

Appl. **9**, 90 (2020).
15. D.E. Chang, V. Vuletić, M.D. Lukin, *Nature Photon.* **8** No 9, 685 (2014).
16. D.G. Lidzey, D.D.C. Bradley, A. Armitage, S. Walker, M.S. Skolnick, *Science.* **288**, 1620 (2000).
17. J. Song, Y. He, A.V. Nurmikko, J. Tischler, V. Bulovic, *Phys. Rev. B.* **69**, 235330 (2004).
18. P. Vasa, R. Pomraenke, G. Cirmi, E.D. Re, W. Wang, S. Schwieger, D. Leipold, E. Runge, G. Cerullo, C. Lienau, *ACS Nano* **4**, 7559 (2010).
19. G.P. Wiederrecht, G.A. Wurtz, J. Hranisavljevic, *Nano Lett.* **4**, 2121 (2004).
20. N.T. Fofang, T. Park, O. Neumann, N.A. Mirin, P. Nordlander, N.J. Halas, *Nano Lett.* **8**, 3481 (2008).
21. O. Ávalos-Ovando, L.V. Besteiro, Z. Wang, A. O. Govorov, *Nanophotonics* **9** No 11, 3587 (2020).
22. Y.H. Qiu, S.-J. Ding, F. Nan, Q. Wang, K. Chen, Z.-H. Hao, L. Zhou, X. Li, Q.-Q. Wang, *Nanoscale.* **11** No 45, 22033 (2019).
23. R.F. Ribeiro, L.A. Martínez-Martínez, M. Du, J. Campos-Gonzalez-Angulo, J. Yuen-Zhou, *Chem. Sci.* **9** No 30, 6325 (2018).
24. Z. He, F. Li, Y. Liu, F. Yao, L. Xu, X. Han, K. Wang, *Appl. Sci.* **10** No 51, 1774 (2020).
25. M.L. Dmytruk, S.Z. Malynych, *Ukr. Fiz. Zh. Ogl.* **9** No 3 (2014) (in Ukrainian).
26. Y. Tang, X. Yu, H. Pan, J. Chen, B. Audit, F. Argoul, S. Zhang, S. Xu, *Appl. Spectrosc.* **71** No 10, 2377 (2017).
27. W. Cao, E.M. Sletten, *J. Am. Chem. Soc.* **140** No 8, 2727 (2018).
28. L. Pol, C. Eckstein, L.K. Acosta, E. Xifré-Pérez, J. Ferré-Borrull, L.F. Marsal, *Nanomaterials* **9** No 3, 478 (2019).
29. K. Tanabe, *Mater. Lett.* **61**, 4573 (2007).
30. A.V. Korotun, V.V. Pogosov, *Phys. Solid State* **63** No 1,

122 (2021).

31. N.A. Smirnova, R.O. Malysh, A.V. Korotun, V.I. Reva, I.M. Titov, *J. Nano- Electron. Phys.* **13** No 5, 05010 (2021).

32. A.V. Korotun, A.O. Koval, V.V. Pogosov, *Ukr. J. Phys.* **66** No 6, 518 (2021).

33. N.I. Grigorchuk, *J. Opt. Soc. Am. B* **29**, 3404 (2012).

34. N.A. Smirnova, M.S. Maniuk, A.V. Korotun, I.M. Titov, *Phys. Chem. Solids State* **24** No 1, 181 (2023).

35. N.I. Grigorchuk, P.M. Tomchuk, *Phys. Rev. B.* **84**, 085448 (2011).

36. V.S. Lebedev, A.G. Vitukhnovsky, A. Yoshidaetal, *Colloids Surf. A* **326** No 3, 204 (2008).

Радіаційна ефективність сферичних металевих наночастинок, вкритих шаром молекулярного адсорбату

А.В. Коротун[1,2], Н.А. Смирнова[1], Г.В. Мороз[1], Г.М. Шило[3]

[1] *Національний університет «Запорізька політехніка», вул. Жуковського 64, 69063 Запоріжжя, Україна*

[2] *Інститут металофізики ім. Г. В. Курдюмова НАН України, бульв. Академіка Вернадського, 36, 03142 Київ, Україна*

[3] *Запорізький національний університет, вул. Жуковського, 66, 69600 Запоріжжя, Україна*

У роботі одержано співвідношення для оптичних характеристик композитних наночастинок типу «металеве ядро – оболонка молекулярного агрегату». Проведено розрахунки частотних залежностей поляризовності, перерізів поглинання та розсіювання, радіаційної ефективності та розмірних залежностей частот гібридних плазмон-екситонних резонансів. Запропоновано наближений підхід до визначення розмірних залежностей частот гібридних плазмон-екситонних мод, суть якого полягає у нехтуванні процесами релаксації в оболонці молекулярного агрегату та металевому ядрі. Продемонстровано, що зі збільшенням радіусу металевого ядра найбільша за величиною частота плазмон-екситонного резонансу зменшується в той час, як наступна за величиною частота збільшується. При цьому найменша з цих частот спочатку зменшується, а коли вміст металевої фракції стає більшим за 50 % від об'єму всієї частинки, починає збільшуватися. Простежено еволюцію максимумів уявної частини поляризовності зі зміною геометричних параметрів композитної наночастинки: радіусу металевого ядра і товщини оболонки. Встановлено, що один із цих максимумів розташований у ближньому ультрафіолетовому діапазоні, тоді як два інших у видимій частині спектра. Крім того, відмічається значне зростання дійсної, уявної частини і модуля поляризовності при збільшенні радіуса металевого ядра. Доведено необхідність врахування як поглинання, так і розсіювання при дослідженні оптичних властивостей наночастинок складу «металеве ядро – оболонка J-агрегату». Показано, що зміни товщини і матеріалу оболонки практично не впливають на величину радіаційної ефективності в оптичному діапазоні частот, в той час як зміна матеріалу і радіусу металевого ядра суттєво впливає на її частотну залежність у видимій області спектра. Встановлена доцільність практичного використання композитних наночастинок із золотим ядром малого радіусу, в яких в усьому оптичному діапазоні частот радіаційна ефективність близька до одиниці.

Ключові слова: Композитні наночастинки, Плазмон-екситонний резонанс, Молекулярний адсорбат, Швидкість релаксації, Частотна залежність.